Chapter 3

N-cadherin mediates aggregation of placodal neurons and may be regulated by Slit1–Robo2 signaling during formation of the cranial ganglia

3.1 Abstract[1]

We have shown in Chapter 2 that in the largest of the cranial ganglia, the trigeminal ganglion, Slit1–Robo2 signaling mediates neural crest–placode interactions and their function is required for proper ganglion assembly. However, the effector molecules that coordinate proper ganglion formation are not known. Furthermore, whether Slit1–Robo2 may also coordinate assembly of the other cranial sensory ganglia has not been examined. Here, we demonstrate a critical role for the cell adhesion molecule N-cadherin downstream of Slit1–Robo2 during gangliogenesis. In the chick embryo, we found that N-cadherin is expressed by placodal neurons in the surface ectoderm and ganglionic anlage of all cranial sensory ganglia, but not by migrating cranial neural crest. Like the trigeminal, epibranchial placodes express the receptor Robo2, whereas the hindbrain neural crest expresses its ligand Slit1, and blocking Robo2 function leads to disorganized epibranchial ganglia. Loss of N-cadherin function in placodal cells results in formation of dispersed ganglia, similar to that observed after loss of Robo2. Perturbing Slit1–Robo2 signaling (increasing Slit1 or reducing Robo2 function) alters N-cadherin expression, suggesting that N-cadherin functions downstream or at least is regulated by Robo2 signaling. Consistent with this, coexpression of full-length N-cadherin partially rescues the Robo2 loss-of-function phenotype. Together, the data suggest a novel and general mechanism whereby Slit–Robo

[1] This chapter is based on the submitted manuscript Shiau CE and Bronner-Fraser M: N-cadherin is linked with Slit1–Robo2 signaling in regulating aggregation of placode-derived cranial sensory neurons.

signaling between neural crest and placodal cells may positively regulate N-cadherin mediated placodal cell adhesion, required for proper ganglion formation in all cranial sensory ganglia of dual origin.

3.2 Introduction

During development, proper formation of various organs and structures requires coordinated interactions between different cell types. In vertebrates, a prime example is the interaction between neural crest and ectodermal placodes, two cell types of distinct embryonic origin, both of which contribute to the ganglia of the head (D'Amico-Martel and Noden, 1983). The cranial sensory ganglia— trigeminal, facial, glossopharyngeal, and vagal— are essential components of the peripheral nervous system that relay sensory information— such as pain, touch, and temperature, from the head and various organs to the brain (Baker, 2005). These ganglia form adjacent and external to the forming midbrain and hindbrain and make central connections to even-numbered rhombomeres (Noden, 1993). Formation of the cranial sensory ganglia requires cell–cell communication that facilitates intermixing, proper positioning, and aggregation of placode and neural crest cells into discrete ganglion structures. However, the signals and the effector molecules that coordinate their proper condensation into the cranial ganglia are largely uncharacterized.

The position and shape of the cranial ganglia largely mirror the migration patterns of the cranial neural crest. Neural crest ablation at the time of trigeminal ganglion assembly demonstrates that this cell type is required for proper organization and integration of

placodal neurons into ganglia (Shiau et al., 2008). Loss of the receptor Neuropilin-2, expressed by neural crest cells, and/or Semaphorin ligands, expressed in the adjacent mesenchyme, cause defects in neural crest migration that lead to malpositioning of neuronal cell bodies and axons. This results in aberrantly interlinked trigeminal and facial ganglia (Gammill et al., 2006; Schwarz et al., 2008). Thus, neural crest cells play a critical role in regulating aggregation of placodal neurons during early ganglion assembly. Cell–cell signaling between neural crest and placodes likely mediates their coordinated and cooperative interactions in forming the cranial ganglia. For example, trigeminal placode cells express Robo2, while neural crest cells express its cognate ligand Slit1. Blocking either receptor or ligand function causes severe malformations such as aberrantly or diffusely condensed ganglia (Shiau et al., 2008).

Slit signaling through Robo receptors plays a broadly conserved role in axon repulsion from the central nervous system midline in both invertebrates and vertebrates (Brose and Tessier-Lavigne, 2000; Dickson and Gilestro, 2006). In addition, Slits and Robos have been implicated in heart tube morphogenesis in the fruit fly, where they appear to regulate cell adhesion and cell polarity genes (MacMullin and Jacobs, 2006; Qian et al., 2005; Santiago-Martinez et al., 2006), including E-cadherin (Santiago-Martinez et al., 2008). In chick neural retinal cultures, as well as mouse fibroblast L-cells that express N-cadherin, Slit activation of Robo appears to inhibit N-cadherin function (Rhee et al., 2002). The cell biological effects downstream of Slit–Robo signaling during vertebrate development are not yet known.

Because cell–cell interactions appear critical for trigeminal ganglion formation, we examined the possible role of the cell–cell adhesion molecule N-cadherin in ganglion assembly and tested for possible links between N-cadherin-mediated adhesion and Robo–Slit signaling. N-cadherin is a member of the type I classical cadherins (as are E-

and R-cadherins). These are transmembrane, Ca^{2+} dependent adhesion molecules that preferentially bind homophilically through the extracellular domains (Gumbiner, 2005). In vertebrates, N-cadherin is expressed in neural crest-derived spinal ganglia (Akitaya and Bronner-Fraser, 1992; Inuzuka et al., 1991; Packer et al., 1997; Redies et al., 1992) and has been implicated in shaping the sympathetic chain ganglia (Kasemeier-Kulesa et al., 2006). N-cadherin is also expressed in sensory fibers at chick stages 29–37 (E6–E11) (Redies et al., 1992) and mouse E12.5 cranial nerves (Packer et al., 1997). However, little is known about its early expression or function during cranial ganglia assembly in amniotes. In zebrafish, N-cadherin appears to be important for cranial ganglia formation (Kerstetter et al., 2004; Liu et al., 2003), though it is not yet clear if it functions in neural crest cells, placodes, or both.

Here, we show that N-cadherin on placode-derived sensory neurons is required for cranial ganglion condensation. Furthermore, knockdown of Robo2 or ectopic expression of Slit1 alters N-cadherin levels and N-cadherin can partially rescue the Robo2 loss-of-function phenotype. Taken together, these data suggest a novel and synergistic relationship between N-cadherin-mediated cell adhesion and Slit1–Robo2 signaling in driving aggregation of placodal neurons into cranial ganglia.

3.3 Materials and methods

Embryos

Fertilized chicken *(Gallus gallus domesticus)* eggs were obtained from local commercial sources and incubated at 37°C to the desired stages according to the criteria of Hamburger and Hamilton (Hamburger and Hamilton, 1992).

In situ hybridization

Whole mount chick in situ hybridization was performed as described (Shiau et al., 2008). cDNA templates used for antisense riboprobes were: chick Slit1 and Robo2 as described (Vargesson et al., 2001). Embryos were imaged and subsequently sectioned at 12 μm.

Immunohistochemistry

Whole chick embryos were fixed in 4% paraformaldehyde overnight at 4ºC, washed in PBT (PBS + 0.2% tween) and either immunostained as whole embryos and/or processed for 10 μm cryostat sections. Primary antibodies used were anti-N-cadherin (DSHB, MNCD2 clone; 1:1), anti-N-cadherin (Abcam; 1:250), anti-GFP (Molecular Probes; 1:1000 to 1:2500), anti-HNK-1 (American Type Culture; 1:3 or 1:5), anti-Islet1 (DSHB, clone 40.2D6; 1:250), and anti-TuJ1 (Covance; 1:250). Secondary antibodies: cyanine 2 or rhodamine red-x conjugated donkey anti-rat IgG (Jackson ImmunoResearch) used at 1:1000 and all others were obtained from Molecular Probes and used at 1:1000 or 1:2000 dilutions (except 1:250 dilution for Alexa Flour 350 conjugated antibodies). Images were taken using the AxioVision software from a Zeiss Axioskop2 plus fluorescence microscope, and processed using Adobe Photoshop CS3.

In ovo electroporation of the trigeminal ectoderm

DNA or morpholino oligomers were injected overlying the presumptive trigeminal placodal ectoderm at stages 8–10 by air pressure using a glass micropipette. Platinum electrodes were placed vertically across the chick embryo delivering 5 × 8 V in 50 ms at 100 ms intervals current pulses. Electroporated eggs were re-sealed and re-incubated at 37˚C to reach the desired stages.

Plasmid constructs and morpholinos

DNA plasmids previously described were used as follows: Robo2Δ-GFP (Hammond et al., 2005), pCMV-cN/CBR(-)/FLAG-pA (pCMV-dn-Ncad) and pCMV-cN/FLAG-pA (pCMV-Ncad) (Nakagawa and Takeichi, 1998), and for control GFP expression, cytoplasmic pCIG (cyto-pCIG) (Shiau et al., 2008) and pCAβ-IRES-mGFP (McLarren et al., 2003). Full-length chick Slit1 cDNA was isolated from a 4– to 12– somite chick macroarray library as described (Gammill and Bronner-Fraser, 2002) for creating the cytopcig-Slit1-LRR construct, which contains the coding sequence for the first 863 amino acids of chick Slit1 with a 3x FLAG tag. The Slit1-LRR-3xFLAG fragment (~2.7 kb) was inserted into cyto-pCIG at XhoI and EcoRI sites. Morpholino oligomer (Gene Tools, LLC) against the start site of chick N-cadherin (Ncad MO) has a 5' –> 3' sequence of: GCGGCGTTCCCGCTATCCGGCACAT. Standard control oligomer from Gene Tools, LLC (control MO) and NCad MO were both 3' lissamine tagged, diluted with water, and used at 1 μM.

3.4 Results

3.4.1 N-cadherin is expressed by trigeminal and epibranchial placodal neurons but not cranial neural crest during gangliogenesis

To determine if N-cadherin is expressed at the right time and place to play a role in cranial gangliogenesis, we examined its expression pattern in the cranial regions of the developing chick embryo from stages 13–17, as the trigeminal and epibranchial ganglia

assemble and aggregate (Fig. 1). Placodal neurons differentiate early, prior to or at the time of ingression (Baker and Bronner-Fraser, 2001; D'Amico-Martel, 1982; D'Amico-Martel and Noden, 1980; Shiau et al., 2008). Neural crest cells migrate to the site of ganglion assembly first but remain undifferentiated as they intermingle with ingressing placodal neurons (Shiau et al., 2008). Neural crest cells begin to differentiate into neurons late in development after the ganglia are well condensed at ~stages 22–24 (D'Amico-Martel and Noden, 1980; D'Amico-Martel and Noden, 1983). Therefore, broad neuronal markers, such as Islet1 and/or β-neurotubulin (TuJ1), uniquely label placodal cells during early ganglion assembly.

During initial ganglion formation, N-cadherin expression is restricted to placode but not neural crest cells. Using immunohistochemistry with antibodies to N-cadherin coupled with HNK-1 to label neural crest cells, and TuJ1 or Islet1 to identify placodal neurons, we observed overlapping expression of N-cadherin with TuJ1 and Islet1 but not with HNK-1 at all stages leading to well-condensed cranial sensory ganglia (Fig. 1), with the exception of a few Islet1 negative cells in the condensed ganglia at stage 17 which express N-cadherin (as an example see Fig. 1I, asterisk). These cells may be non-Islet1 expressing placodes or mesenchymal cells of mesoderm or neural crest origin. N-cadherin staining was apparent both in the placodal ectoderm as well as in those placode cells that have ingressed; expression continued through the time of cranial ganglia assembly (Fig. 1). Consistent with previous reports, we also found high levels of N-cadherin expression in the neural tube, notochord, and the lens (Hatta et al., 1987; Hatta and Takeichi, 1986), and slightly lower levels in the mesoderm-derived mesenchyme. The intensity of immunostaining in placodal cells is generally lower than in the neural tube, and is more similar to that in the mesenchyme cells.

Interestingly, N-cadherin levels fluctuate dynamically in placodal tissue as a function of time. In the trigeminal region, at times of early ingression at stage 13, N-

cadherin is expressed in most of the surface ectoderm around the head, with the exception of the region overlying the dorsal hindbrain (Fig. 1A,B). Later by stages 15–17, expression is mostly down-regulated in the ectoderm overlying the site of ganglion assembly (Fig. 1C-E), though the ectoderm that overlies the frontonasal region (including the lens) still expresses N-cadherin (data not shown). The discrete spots of low-level expression in the surface ectoderm later in development may correlate with sites of placode ingression, which continues through stage 21 (D'Amico-Martel and Noden, 1983), well after the ganglion is condensed. The expression of N-cadherin in the ingressed placodal neurons appears to increase with time and change from a punctated to a more continuous cell surface expression from stage 13 (Fig. 1A,B) to 17 (Fig. 1C-G) as the trigeminal ganglion is condensing. Similar to the trigeminal placode, we observed N-cadherin expression in the epibranchial ectoderm and ingressing epibranchial placodes (Fig. 1H-P). The expression of N-cadherin by placodal neurons in all cranial ganglia raises the possibility that N-cadherin may play a general role in placodal ingression and/or aggregation.

3.4.2 Loss of N-cadherin phenocopies Robo2 loss-of-function

To test the possible function of N-cadherin in placode cells during gangliogenesis, we focused on the forming trigeminal ganglion because of its large size and characteristic semilunar shape, which aids in systematic scoring of ganglionic phenotypes. To deplete N-cadherin in the placodal cells, we used both a translation blocking antisense morpholino oligomer (MO) against chick N-cadherin (Ncad MO) and a dominant-negative N-cadherin construct (pCMV-dn-Ncad) (Nakagawa and Takichi, 1998) which encodes chick N-cadherin lacking the intracellular β-catenin binding domain. Such mutations to cadherins lacking binding site to β-catenin have been shown to block cadherin function (Nakagawa and Takeichi, 1998; Shoval et al., 2007).

The effects of both knockdowns were similar but Ncad MO gave a more pronounced phenotype, giving rise to highly dispersed placodal neurons in the forming ganglia at stages 15–16 (29% severe and 42% mild defects, n=24) and in largely misshapen ganglia at later stages 17–18 (8% severe and 23% mild, n=13) after the ganglion is well condensed (Fig. 2B,E). In contrast, control MO embryos showed little or no effect (Fig. 2A,E). The effects of dispersed and disorganized placodal neurons (both cell bodies and axon projections) in the forming trigeminal ganglion observed with Ncad MO were reminiscent of the defects caused by Robo2 loss-of-function using the Robo2Δ-GFP construct (Shiau et al., 2008) which encodes a dominant-negative Robo2 that lacks its intracellular tail, replaced by the GFP. However, defects in axon guidance were more pronounced in Robo2 deficient embryos.

The effectiveness of Ncad MO in depleting N-cadherin protein was confirmed using immunohistochemistry in the neural tube and lens, where N-cadherin expression is persistent and strong. Chick embryos electroporated with Ncad MO in these tissues showed a marked reduction of N-cadherin protein as compared with control MO embryos (Fig. 3). Similar reductions were observed in the trigeminal region (Fig. 5). Ncad and control MOs were tagged with 3' lissamine for detection.

Similar to but less severe than the Ncad MO, pCMV-dn-Ncad electroporated embryos resulted in dispersed trigeminal ganglion at early ganglion assembly (stages 15–16) (7% severe and 40% mild phenotypes, n=19) (Fig. 2C-E). In contrast to the MO, dn-Ncad protein expression driven by pCMV-dn-Ncad appeared to incorporate rather mosaically. Expression levels were checked by co-electroporating pCMV-dn-Ncad with a control GFP vector. In these embryos, we detected dn-Ncad-FLAG expression in only a sub-population of transfected GFP expressing cells (Fig. 4), perhaps accounting for the milder defects observed with this construct as compared to the Ncad MO. These results

show that placodal neurons require N-cadherin function for proper ganglion condensation in common with Robo2 function.

3.4.3 N-cadherin is essential for ganglion condensation, but not placodal ingression

Since N-cadherin is expressed dynamically in both the surface ectoderm from which placodal cells arise and in the ingressing placodal cells after detaching from the ectoderm, we asked whether N-cadherin is critical for placodal ingression. To this end, we counted the total number of placodal cells (Islet1+) in 10 μm frontal sections collected from the entire presumptive trigeminal region at times of early and abundant ingression at stage 14 (boxed region in Fig. 5) and analyzed the number associated with the surface ectoderm (either in ectoderm or adjacent to its basal margin) versus the mesenchyme as previously described (Shiau et al., 2008). These two categories represent the population of placodal neurons that are undergoing ingression or preparing to do so, and those that have already ingressed, respectively. In contrast to the effect of Robo2 inhibition that caused more than a two-fold increase in percentage of placodal cells remaining associated with the ectoderm than those in controls (Shiau et al., 2008), we found no significant difference between the numbers of ingressing cells in Ncad loss-of-function (36.3 ± 3.9%, n=3) versus control (32.2 ± 7.6%, n=4) embryos (Fig. 5A-C). Furthermore, the total number of Islet1+ placodal cells was not significantly different between Ncad MO and control MO embryos, suggesting no effect on placodal cell number when N-cadherin is reduced. This suggests that Robo2 dependent ingression process does not rely on N-cadherin. On the other hand, the placodal cells appear more dissociated in Ncad MO embryos (Fig. 5B,C). Thus, N-cadherin appears to be one of several downstream mediators and interacting partners of Slit1–Robo2 signaling. However, we cannot rule out that the efficiency of Ncad MO

mediated knockdown is not sufficient to reveal an early role for N-cadherin during ingression.

In contrast to these early stages, significant alterations were noted in Ncad MO mediated ganglion compared with controls during ganglion assembly (stage 16). The results suggest that loss of N-cadherin in placodal cells reduces cell–cell contact and abrogates clustering of placodal neurons (Fig. 5D,E). Ncad MO placodal neurons appear dissociated and have reduced levels of N-cadherin expression (Fig. 5E). These results are consistent with the dispersed ganglia observed in whole-mount. Though N-cadherin deficient placodal cells are more dispersed, they generally occupy the same approximate area within the head mesenchyme where the trigeminal ganglion forms, in close proximity to the surface ectoderm (Fig. 5E). Thus, knockdown of N-cadherin appears to compromise placode–placode cell association and aggregation, but not ingression or ganglion position.

3.4.4 Perturbation of Slit1–Robo2 signaling can alter N-cadherin expression

The similar loss-of-function phenotypes of both N-cadherin and Robo2 raise the intriguing possibility that they may function in the same pathway to mediate interactions between placodal neurons in the forming ganglion. To test this, we first examined the effects of Slit1–Robo2 signaling on N-cadherin in placodal cells and asked whether blocking or activating Slit1–Robo2 signaling would alter N-cadherin expression. The results show that inhibiting Robo2 signaling by Robo2Δ-GFP causes down-regulation of N-cadherin expression in the placodal ectoderm at stages 13–14 at times of early ingression (Fig. 6A). Later, at stage 17, there was a reduction of N-cadherin expression in aberrantly dispersed individual placodal neurons in the forming ganglion (Fig. 6E-G). However, many of the Robo2Δ-GFP placodal neurons still express some levels of N-cadherin, particularly

ones that appear more closely associated with each other. Thus, Robo2 may modulate N-cadherin expression but is unlikely to be the sole regulator of N-cadherin in placodal cells.

Conversely, to test the effects of Slit activation of Robo on N-cadherin, we designed a construct encoding the N-terminal portion of chick Slit1, that encompasses the four leucine rich repeats (cytopcig-Slit1-LRR), which has been shown to be sufficient for binding and activating Robo (Morlot et al., 2007, Howitt et al., 2004, Chen et al., 2001, Battye et al., 2001), and more potent than full length Slit to rescue midline axon defect in fly slit mutants (Battye et al., 2001). cytopcig-Slit1-LRR was introduced into the placodal ectoderm by in ovo electroporation to test the effect of Slit1 expression in placodal cells on N-cadherin expression. Strikingly, ectopic expression of Slit1 in the placodal ectoderm causes aberrant placodal aggregates in the forming trigeminal ganglion (44% at stages 15–16 with n=9 and 31% at stages 17–18 with n=13 showing severe defects in condensation, including ectopic aggregates and/or axonal disorganizations) (Fig. 7F-L). Furthermore, in these ganglia, we found that N-cadherin expression was up-regulated in discrete regions of the surface ectoderm corresponding to locations near aberrant placodal clusters (Fig. 7J) at times when N-cadherin is normally down-regulated in the surface ectoderm, as seen in stage 16 GFP control embryos (Fig. 7E). This defect was more severe in the ophthalmic (OpV) than in the maxillomandibular (MmV) region of the forming ganglion, consistent with our previous finding that Robo2 inhibition has more severe effects on the OpV (Shiau et al., 2008). Thus, the effect of ectopic Slit1 expression on N-cadherin is reciprocal to that of blocking Robo2, consistent with the idea that N-cadherin is positively regulated by Slit1–Robo2. Taken together, inhibition of Robo2 or its activation by Slit1 can either decrease or increase N-cadherin expression respectively, suggesting that Slit1–Robo2 interaction can modulate N-cadherin expression.

3.4.5 Overexpression of N-cadherin partially rescues Robo2 perturbation

The observation that Robo2 loss-of-function leads to reduction of N-cadherin suggest that N-cadherin is downstream of and may be epistatic to Robo2. To test whether N-cadherin can rescue the effects of Robo2 inhibition in the placodal cells, we co-electroporated full length N-cadherin (pCMV-Ncad) and Robo2Δ-GFP into the placodal ectoderm. Despite its mosaic expression (similar to pCMV-dn-Ncad described above), the results show that N-cadherin partially rescues the severely dispersed ganglion phenotype of Robo2 inhibition at stages 15–16 by about 18% (n=8, Fig. 8A-C). Embryos co-electroporated with pCMV-Ncad and Robo2Δ-GFP had ganglia that were markedly less dispersed and more coalesced than those with Robo2Δ-GFP alone. In contrast, N-cadherin gain-of-function alone, achieved by electroporating pCMV-Ncad with a control GFP vector to visualize DNA incorporation into the placodal ectoderm, had no obvious effects on ganglion organization, yielding rather normal (87%, n=15) or slightly smaller (13%, n=15) ganglia (data not shown). All together, results show that N-cadherin can act downstream of Robo2 signaling as its gain-of-function compensates for the effects of blocking Robo2 and Slit1–Robo2 signaling modulates N-cadherin expression.

3.4.6 Robo2–Slit1 and N-cadherin expression and function are common to trigeminal and epibranchial regions

Since Slit1–Robo2 interactions have been implicated in assembly of the trigeminal ganglion (Shiau et al., 2008), we asked whether this receptor/ligand pair may generally function in neural crest–placode assembly of all cranial sensory ganglia. To this end, we further characterized the expression patterns of Robo2 and Slit1 in the hindbrain regions of the chick embryo during epibranchial gangliogenesis at stages 16–18. The results show that

the complementary expression pattern of Robo2 in the placodes and its ligand Slit1 in the neural crest is common to all forming epibranchial ganglia. By in situ hybridization coupled with immunohistochemistry with the neural crest marker HNK-1, we find that all epibranchial placodes (geniculate, petrosal, and nodose corresponding to the facial, glossopharyngeal and vagal ganglia respectively) express Robo2 mRNA during early assembly at stage 16 (Fig. 9A) and continue expression up to ganglion condensation at stage 18 (Fig. 9B), while the migratory hindbrain neural crest at rhombomeres 4 and 6 expresses Slit1 mRNA at stage 16 (Fig. 9C) and begins to down-regulate Slit1 expression at stage 18 (Fig. 9D) after the ganglia have condensed. Robo2 also is expressed in the otic placode as previously reported (Battisti and Fekete, 2008) and in parts of the ectoderm surrounding the branchial arches.

Transverse sections reveal that Robo2 expressing cells in the ectodermal and ingressing placodes intermingle with HNK-1 positive migratory neural crest cells that coexpress Slit1 at stage 16 in the forming facial ganglion (Fig. 9E-H) and glossopharyngeal ganglion (Fig. 9I-L). Furthermore, blocking Slit–Robo signaling by introducing Robo2Δ-GFP into the epibranchial placodal cells led to disorganization of the epibranchial placodal ganglia similar to the effects in the trigeminal ganglion (Fig. 9M). Similar to Robo2 inhibition, N-cadherin depletion by Ncad MO in the epibranchial placodes caused a more pronounced effect on the central axonal projections to the hindbrain than in the trigeminal region (Fig. 9N). The central projections in the forming trigeminal ganglion are generally not affected upon Robo2 or N-cadherin perturbation. This could reflect the difference in the cell movements and integration of trigeminal versus epibranchial placodal neurons into ganglia, as the latter forms more distal to the hindbrain. Nevertheless, these results highlight the intriguing possibility that Slit1–Robo2 signaling and N-cadherin function may be a general mechanism for neural crest–placode interaction during cranial gangliogenesis.

3.5 Discussions

3.5.1 Cross-talk between Slit–Robo and cadherins

Our results suggest a novel mechanism in chick cranial gangliogenesis whereby Slit1–Robo2 signaling between neural crest and placodal cells regulates adhesion of placodal neurons via modulation of N-cadherin levels. Recent in vitro studies (Rhee et al., 2007; Rhee et al., 2002) show that Slit activation of Robo causes phosphorylation of β-catenin by Robo-bound Abelson (Abl) tyrosine kinase, thus inhibiting N-cadherin's link to the actin cytoskeleton. In vivo studies in *Drosophila* demonstrate that Slit–Robo signaling inhibits E-cadherin to allow cell shape changes for lumen formation in the developing heart tube (Santiago-Martinez et al, 2008). Contrasting with this negative regulation of cadherins, our data in vertebrates suggests that Slit–Robo signaling can also positively regulate cadherin mediated cell adhesion during chick cranial gangliogenesis. Since this receptor–ligand pair can mediate both repulsive and attractive functions in cell migration and axon patterning (Chedotal, 2007), it may not be too surprising that Slit–Robo may both positively and negatively regulate cadherin mediated adhesion, in a context dependent manner. This may depend on the target tissue, the presence or absence of interacting molecules, and the levels of Slit signaling. The mechanism by which Slit binding to Robo transduces downstream signaling remains an unresolved question, but has been proposed to involve the state of oligomerization of Robo and recruitment of cytosolic adaptor proteins (Hohenester, 2008).

3.5.2 Role of N-cadherin in cellular condensation and its link with Slit1–Robo2

The dynamic expression pattern of N-cadherin in various developing tissues (nervous system, connective tissues, somite, limb, lung, kidney, and heart) undergoing morphogenesis suggests a potentially general role for this cell adhesion molecule in cellular condensation and/or organ formation (Duband et al., 1987; El Sayegh et al., 2007; Hatta et al., 1987). N-cadherin has been found to promote coalescence in the forming heart, somite and limb mesenchyme (Linask et al., 1998; Oberlender and Tuan, 1994; Radice et al., 1997). Accordingly, we find that N-cadherin function is essential for condensation of placodal neurons into cranial ganglia. Our data further suggest a role for Slit1–Robo2 in regulating N-cadherin expression in placodal neurons. However, there are likely to be many other regulators of N-cadherin as its expression is broad in the surface ectoderm and other tissues. Consistent with this, blocking Slit–Robo signaling by Robo2Δ-GFP does not completely eliminate N-cadherin expression in the placodal cells. Interestingly, the more severe defects in trigeminal placodal ingression and axonal projections observed in Robo2 deficient embryos cannot be completely explained by N-cadherin loss-of-function, which affects ganglion condensation but seemingly not ingression or axonal pathfinding. Thus, other yet unknown effector molecules may mediate Slit1–Robo2 signaling in conjunction with N-cadherin, and N-cadherin likely also has independent functions in the placodal ectoderm. Nonetheless, the similarity of the ganglionic loss-of-function phenotype of both N-cadherin and Robo2, together with the partial rescue of Robo2 inhibition by full-length N-cadherin and the changes in N-cadherin expression caused by altering Slit1–Robo2 signaling, combine to provide strong evidence for modulation of N-cadherin by Robo2 dependent signaling in trigeminal placodal aggregation.

3.5.3 Possible mechanisms on how Slit1–Robo2 regulate N-cadherin

How does Slit1–Robo2 regulate N-cadherin expression and/or function in the placodal cells? One possibility is that this is mediated by convergence of common or interacting intracellular molecules involved with both Robo2 and N-cadherin functions, such as the small Rho GTPases (Rho, Rac, Cdc42) that regulate the actin cytoskeleton. Cadherins have been known to not only act as cell adhesion proteins but also as signaling molecules that can elicit changes to intracellular signals (Yap and Kovacs, 2003). Both Robo (Chedotal, 2007; Ghose and Van Vactor, 2002; Guan and Rao, 2003) and cadherin (Charrasse et al., 2002; Noren et al., 2001; Yap and Kovacs, 2003) signaling have been shown to regulate Rho GTPases, which conversely can feedback on cadherin (Braga, 1999; Fukata and Kaibuchi, 2001). Slit signaling can upregulate a Rho family member, Rac1, in the *Drosophila* CNS midline (Fan et al., 2003), and increased Rac1 expression upregulates N-cadherin expression during chondrogenesis (Woods et al., 2007). Therefore, an intriguing possibility is that activation of Rac1 by Slit–Robo may promote N-cadherin expression. The relationship between cadherins and Rho GTPases is likely complex and bi-directional. The effects of Rho and Rac signaling on cadherins have been found to vary for different cadherin subtypes and cellular contexts (Braga et al., 1999). Conversely, cadherins can affect Rho GTPases. For example, a recombinant Fc fused cadherin ectodomain that activates cadherin adhesion causes a rapid increase of Rac activity (Kovacs et al., 2002; Noren et al., 2001). Thus, like Robo signaling, cadherins can regulate Rac, suggesting a point of cross-talk between Robo and cadherin signaling. Independently, Robo2 may regulate other intracellular associations of N-cadherin, such as the catenins, by phosphorylation to promote and/or inhibit cadherin function. Consistent with this possibility, p120-catenin has been shown to stabilize cadherins and regulate their turnover at the cell surface (Kowalczyk and Reynolds, 2004; Perez-Moreno and Fuchs, 2006).

3.5.4 General mechanism involving Slit1–Robo2 and N-cadherin in cranial sensory gangliogenesis in chick

The common expression of Robo2 and N-cadherin in the trigeminal and epibranchial placodes and Slit1 in all migratory cranial neural crest streams underscores a possible general mechanism in mediating neural crest–placode interactions in all cranial sensory ganglia. During development, the trigeminal ganglion forms adjacent to the midbrain while the epibranchial (facial, glossopharyngeal and vagal) ganglia form around the second to the fourth branchial arches, respectively. Epibranchial ganglia have a long tubular-like morphology distinct from the bi-lobed shape of the trigeminal ganglion. However, at times of early cell assembly, the two regions have many similarities. The distribution of neural crest- and placode- derived cells in the trigeminal and epibranchial ganglia is very similar in that neural crest cells intermix with placodal neurons and the most proximal regions of the ganglia are solely neural crest-derived (Begbie and Graham, 2001a; Shiau et al., 2008). Neural crest ablations in both regions cause aberrant projection patterns of placode-derived neurons (Begbie and Graham, 2001a; Shiau et al., 2008). In addition, Slit1 is expressed by neural crest cells in the epibranchial region in a discrete time window correlating with ganglion assembly as is the case in the trigeminal region (Shiau et al., 2008). Slit1 is down-regulated in the hindbrain neural crest after stage 16, slightly later than in the midbrain, likely reflecting the rostral to caudal order of ganglion development from trigeminal to epibranchial gangliogenesis. Functional perturbations of Robo2 and N-cadherin in the epibranchial placodes led to ganglion disorganization, which further lend support for the common mechanism of Slit1–Robo2 mediated neural crest–placode assembly of ganglion.

3.5.5 Expression of N-cadherin may not be placode-specific but rather neuronal cell type-specific in the forming ganglia

The expression and function of N-cadherin in placodal cells but not in cranial neural crest cells probably relates to the state of neuronal differentiation rather than the precursor cell type within the ganglia. Since cranial neural crest cells differentiate into neurons (D'Amico-Martel, 1982; D'Amico-Martel and Noden, 1980) much later in development than placode cells, well after the cranial ganglia have formed, they may not begin to express N-cadherin until past gangliogenesis. In support of this, at trunk levels, which lack placodal cells, N-cadherin is expressed in all neural crest-derived peripheral ganglia- dorsal root and sympathetics (Akitaya and Bronner-Fraser, 1992; Kasemeier-Kulesa et al., 2006). As at cranial levels, migrating trunk neural crest cells do not express N-cadherin until after they have begun to coalesce and differentiate into neurons (Akitaya and Bronner-Fraser, 1992).

3.5.6 Conclusions

In summary, the present results show that N-cadherin plays a crucial role in driving aggregation of placodal neurons and may be regulated by Slit1–Robo2 interactions between neural crest and placodal cells during trigeminal gangliogenesis. This represents the first in vivo evidence of a functional link between cadherin and Slit–Robo signaling in vertebrate development. The similar expression patterns of these molecules in all cranial ganglia suggest a possible general mechanism whereby Slit–Robo signaling controls morphogenesis associated with cadherin function in forming cranial sensory ganglia. Beyond the nervous system, Slits and Robos are emerging as important players in development of the lung, mammary gland, and kidney, as well as pathological conditions

such as cancer and inflammation (Hinck, 2004; Legg et al., 2008; Piper and Little, 2003), where cadherins are also expressed (Hatta et al., 1987; Jeanes et al., 2008; Knudsen and Wheelock, 2005; Stemmler, 2008). The results demonstrate the importance of heterotypic cell interactions during condensation of the cranial sensory ganglia, and implicate a possibility for cross-talk between Slit–Robo signaling and cadherin function in other systems.

3.6 Acknowledgements

I thank Masatoshi Takeichi for the pCMV-dn-Ncad and pCMV-Ncad plasmids and Meyer Barembaum for critical reading and comments. This work was supported by US National Institutes of Health (NIH) National Research Service Award 5T32 GM07616 to C. E. S. and NIH grant DE16459 to M.B.-F.

Figure 1.

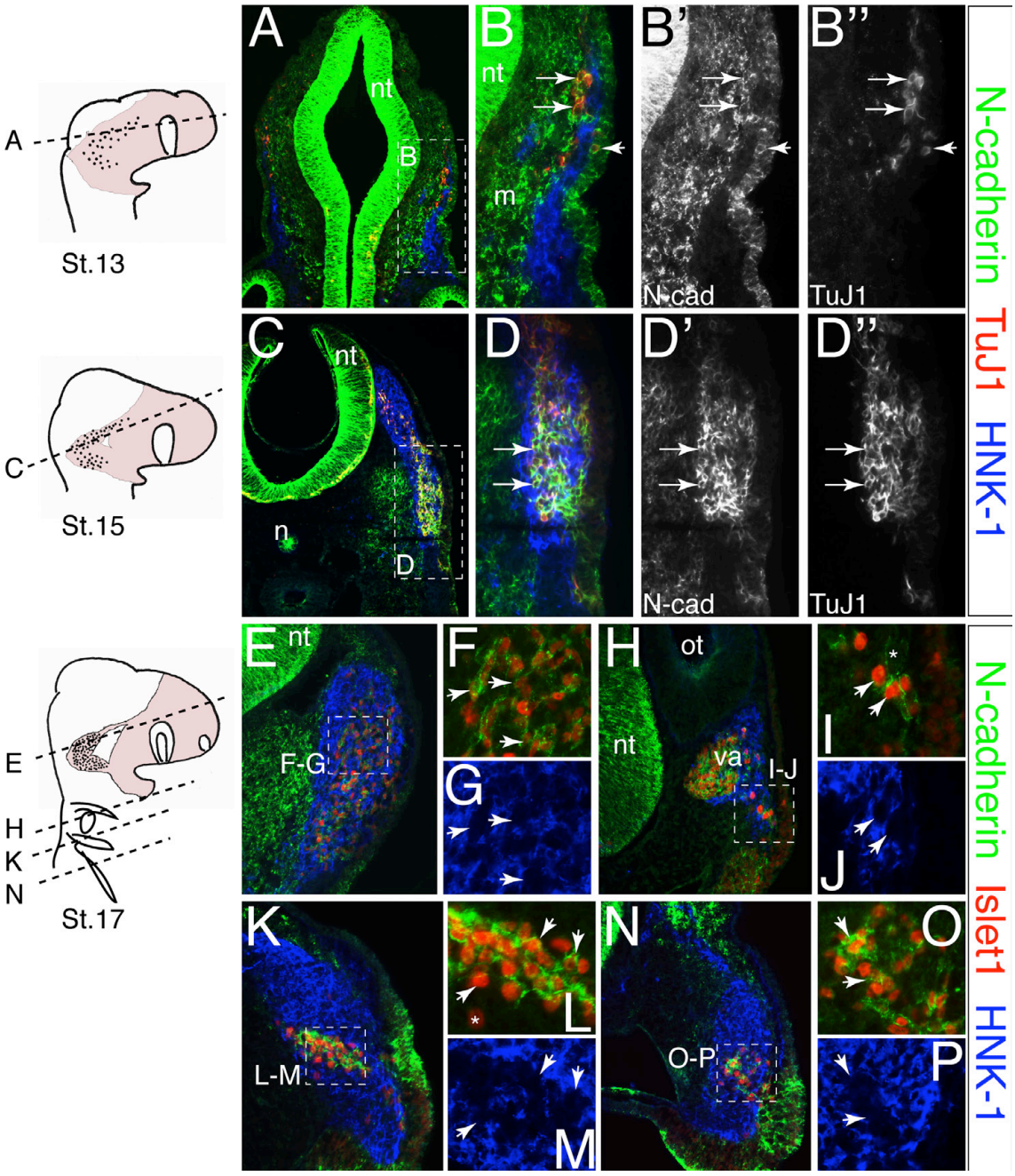
A
St.13
C
St.15
E
H
K
N
St.17
A
nt
B
B
nt
m
B'
N-cad
B''
TuJ1
C
nt
n
D
D
D'
N-cad
D''
TuJ1
N-cadherin TuJ1 HNK-1
E
nt
F-G
F
G
H
ot
nt
va
I-J
I
*
J
K
L-M
L
*
M
N
O-P
O
P
N-cadherin Islet1 HNK-1

Figure 1. Expression of N-cadherin in trigeminal and epibranchial placodal cells but not cranial neural crest during gangliogenesis. Through stages of gangliogenesis, N-cadherin protein is expressed by placodal neurons (labeled by TuJ1 or Islet1) but not by neural crest cells (labeled by HNK-1) in the forming trigeminal ganglion at (**A**) stage 13 with higher magnification of boxed area in **B**, **B**' and **B''** showing coexpression of N-cadherin and TuJ1 (arrows), (**C–D''**) stage 15 in early forming ganglion showing overlap of N-cadherin and TuJ1 (arrows) and (**E–G**) stage 17 in the well condensed ganglion (arrows). Expression of N-cadherin in epibranchial neurons (Islet1+) but not the neural crest cells (HNK-1+) is shown in the (**H–J, arrows**) facial (or geniculate), (**K–M, arrows**) glossopharyngeal (or petrosal), and (**N–P, arrows**) vagal (or nodose) ganglionic regions. By stage 17, a few cells Islet1 negative cells were found to express N-cadherin in the condensing ganglia at stage 17 (**I**, asterisk). The vast majority of Islet1 positive placodal cells express N-cadherin with a few exceptions (**L**, asterisk). All images are derived from 10 μm cryostat sections which generally encompass about one to two cell layer thickness. Schematics of the stage 13, 15, and 17 chick embryos show the levels of the sections with pink area representing the neural crest cells and black dots the placodes. N-cad, N-cadherin; nt, neural tube; m, mesoderm; n, notochord; ot, otic vesicle; va, vestibuloacoustic ganglion.

Figure 2.

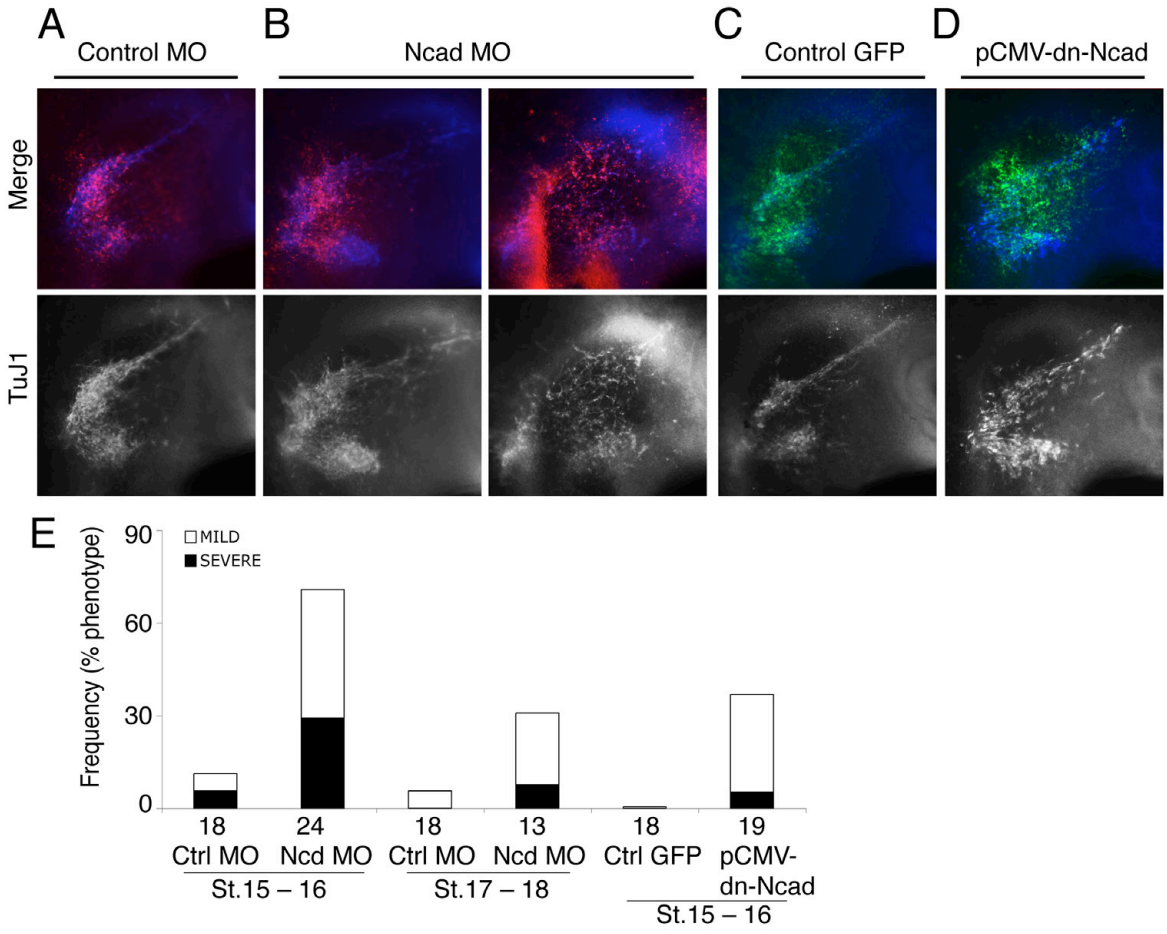
A
Control MO
B
Ncad MO
C
Control GFP
D
pCMV-dn-Ncad
Merge
TuJ1
E
MILD
SEVERE
Frequency (% phenotype)
90
60
30
0
18
Ctrl MO
24
Ncd MO
18
Ctrl MO
13
Ncd MO
18
Ctrl GFP
19
pCMV-dn-Ncad
St.15 – 16
St.17 – 18
St.15 – 16

Figure 2. N-cadherin loss-of-function phenocopies Robo2 loss-of-function. (**A**) Control morpholino electroporated chick embryos in the trigeminal placodal ectoderm analyzed at stage 16 have normal morphology. (**B**) In contrast, stage 16 Ncad MO embryos showed either mildly dispersed and/or misshapen (left) or severely dispersed and disorganized (right) ganglia (TuJ1+). Control and Ncad morpholinos are labeled by 3' lissamine (red in color overlay panels). Compared to (**C**) GFP controls, (**D**) pCMV-dn-Ncad embryos also resulted in aberrantly dispersed placodal ganglia, though less severe than the Ncad MO effects. (**E**) Histogram of data shows the high percentage of dispersed ganglia defects in Ncad MO and dn-Ncad embryos above controls. The more severe effects of Ncad MO at stages 15–16 than at later stages 17–18 likely is due to dilution of morpholino in the placodes over time. Numbers below bar graphs represent the number of transfected ganglia analyzed. Ganglia phenotypes scored as "mild" means misshapen, slight cell dispersion, and/or regional severe defects (in only part of the transfected area), and "severe" means widespread dispersion in most transfected area, including the interlobic region, and/or strikingly aberrant placodal condensation. Ctrl, control; Ncd, N-cadherin.

Figure 3.

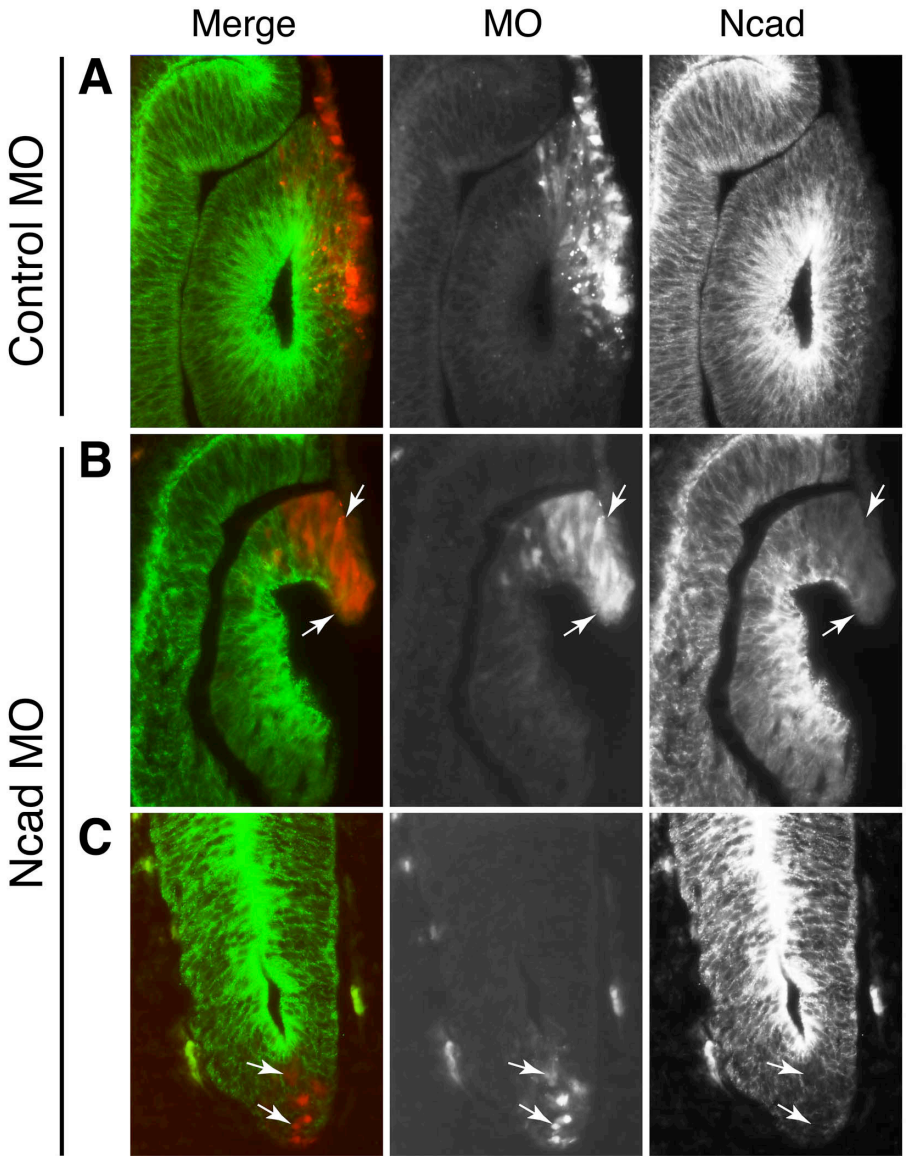

Figure 3. Ncad morpholino is effective in depleting the N-cadherin protein. In contrast to (**A**) the control MO, Ncad MO is effective in blocking translation of N-cadherin protein in the (**B**) lens and (**C**) neural tube where N-cadherin expression is high and persistent, as shown by loss of N-cadherin expression (green; also shown in right panel) in Ncad MO cells (red; also shown in middle panel).

Figure 4.

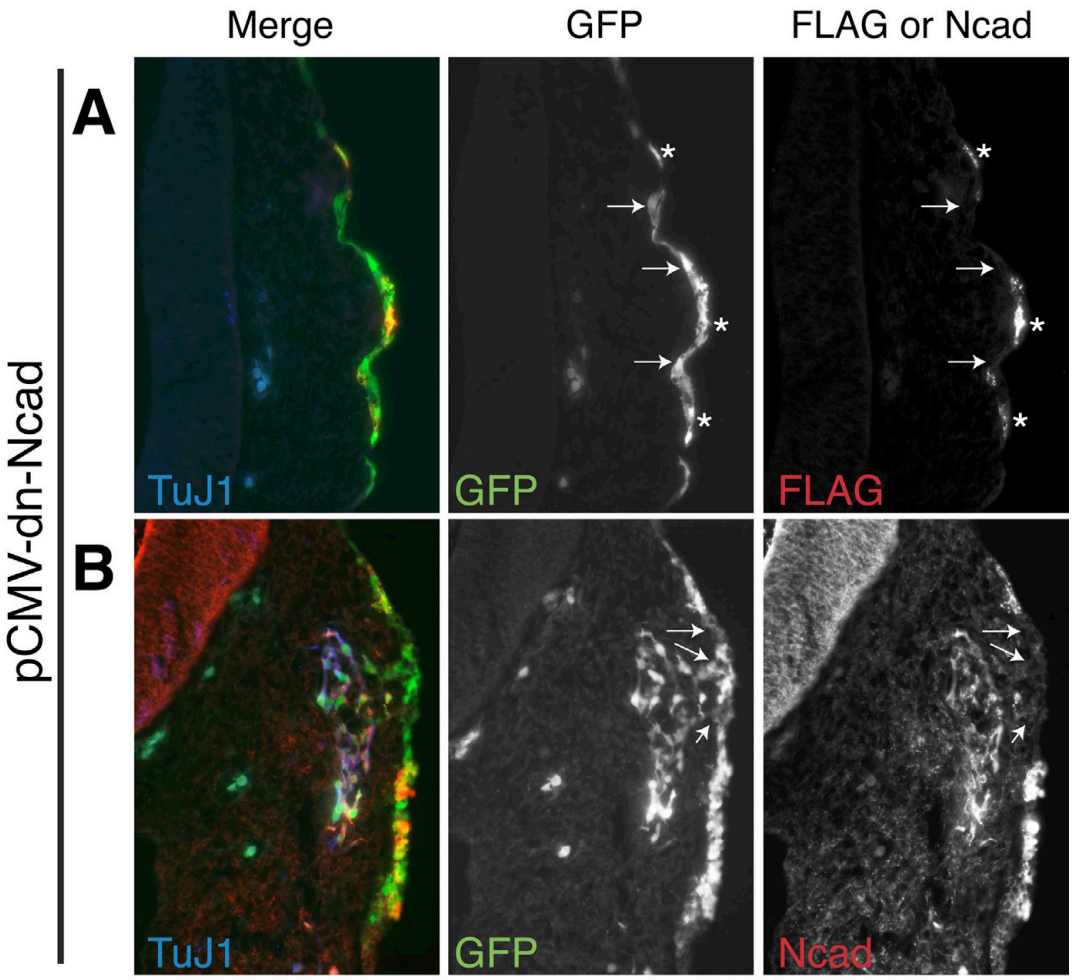

Figure 4. pCMV-dn-Ncad expression leads to mosaic dn-Ncad protein expression. Placodal cells co-electroporated with a control GFP vector and pCMV-dn-Ncad do not all express the dn-Ncad protein. Not all GFP expressing cells express the dn-Ncad protein as visualized by (**A**) the FLAG epitope which is fused to the dn-Ncad (arrows), instead only a subpopulation does (asterisk). (**B**) Similar results were observed using the MNCD2 antibody which recognizes the extracellular domain of N-cadherin and can also detect dn-Ncad; arrows show cells that express GFP but not dn-Ncad. Nonetheless, a large population of the electroporated cells do express the dn-Ncad protein.

Figure 5.

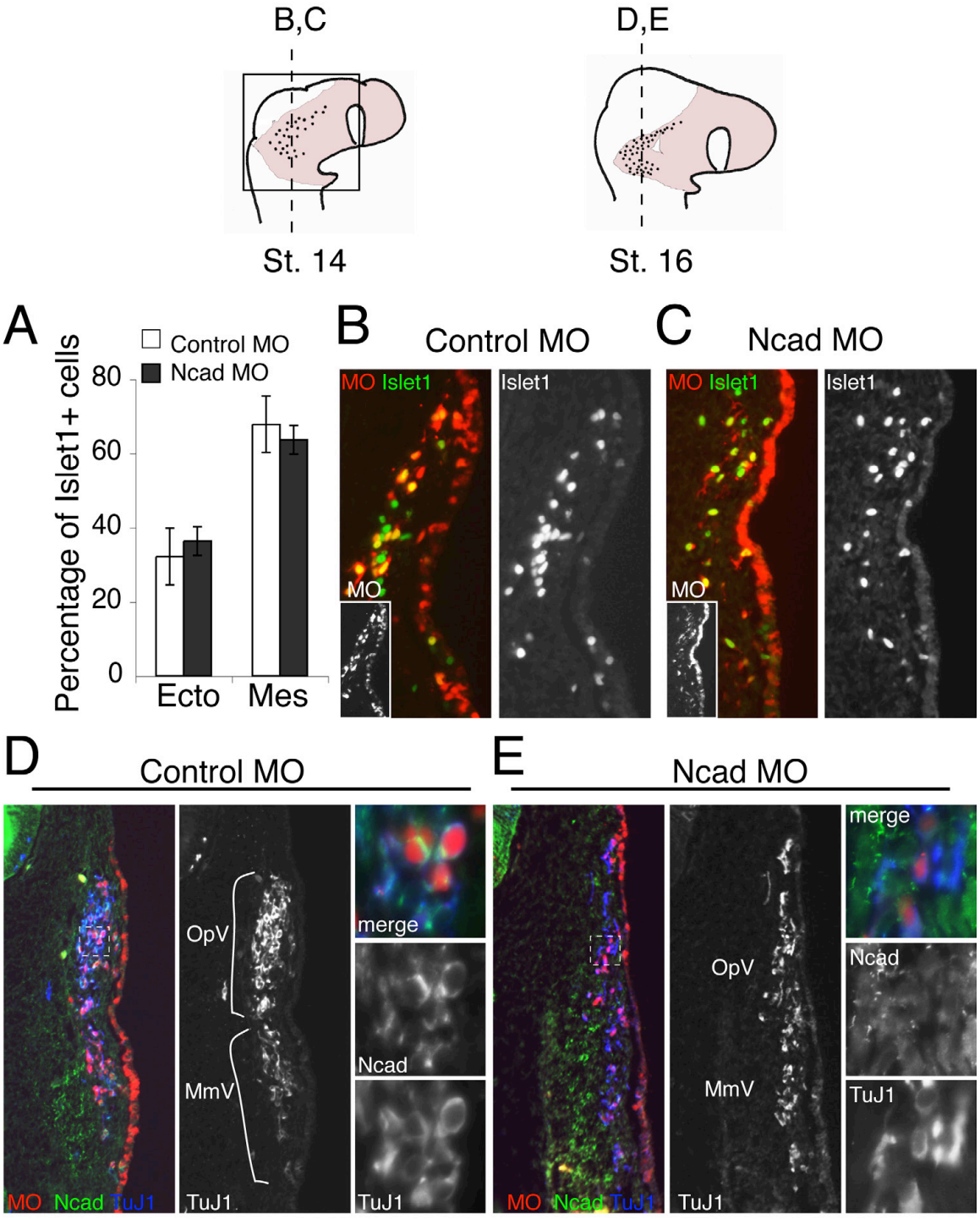
B,C
D,E
St. 14
St. 16
A
Control MO
Ncad MO
Percentage of Islet1+ cells
80
60
40
20
0
Ecto
Mes
B
Control MO
C
Ncad MO
MO Islet1
Islet1
MO
D
Control MO
E
Ncad MO
OpV
MmV
merge
Ncad
TuJ1
MO Ncad TuJ1

Figure 5. N-cadherin is required for placodal condensation, but not ingression. (**A**) Histogram shows that the percentages of Islet1+ placodal cells associated with ectoderm or in the mesenchyme between control MO (n=4) and Ncad MO (n=3) embryos were not significantly different, suggesting that N-cadherin may not be required for ingression. (**B**, **C**) Left, color overlay of MO transfection (red and inset) and Islet1 (green) expression on placodal cells, and right, single channel image of Islet1 of the same section. Compared to (**B**) control MO embryos, placodal cells in the (**C**) Ncad MO embryos appear more scattered early on during ingression at stage 14. (**D**, **E**) Left, color overlay of MO (red), N-cadherin (green), and TuJ1 (blue) on placodal cells; middle, single channel of TuJ1 of the same section; right column of panels, high magnification images of the dotted boxed region in color overlay panels (left). (**D**) Frontal plane section through a stage 16 control MO embryo shows beginning of coalescence of placodes into distinct OpV and MmV lobes (demarcated by white brackets). High magnification of the boxed region shows that these control MO placodal cells retain N-cadherin expression and appear clustered as revealed by TuJ1. (**E**) By contrast, Ncad MO placodal cells appear abnormally dispersed and the OpV and MmV lobes are not easily distinguishable. High magnification of the boxed region shows that these cells have reduced or no N-cadherin expression and have less cell contacts with one another. Schematic of stage 14 chick embryo shows the boxed region of analysis for placodal ingression and the level of sections in **B** and **C** and stage 16 chick embryo schematic shows the level of sections in **D** and **E**. Ecto, ectoderm associated; Mes, mesenchyme; OpV, ophthalmic; MmV, maxillo-mandibular.

Figure 6.

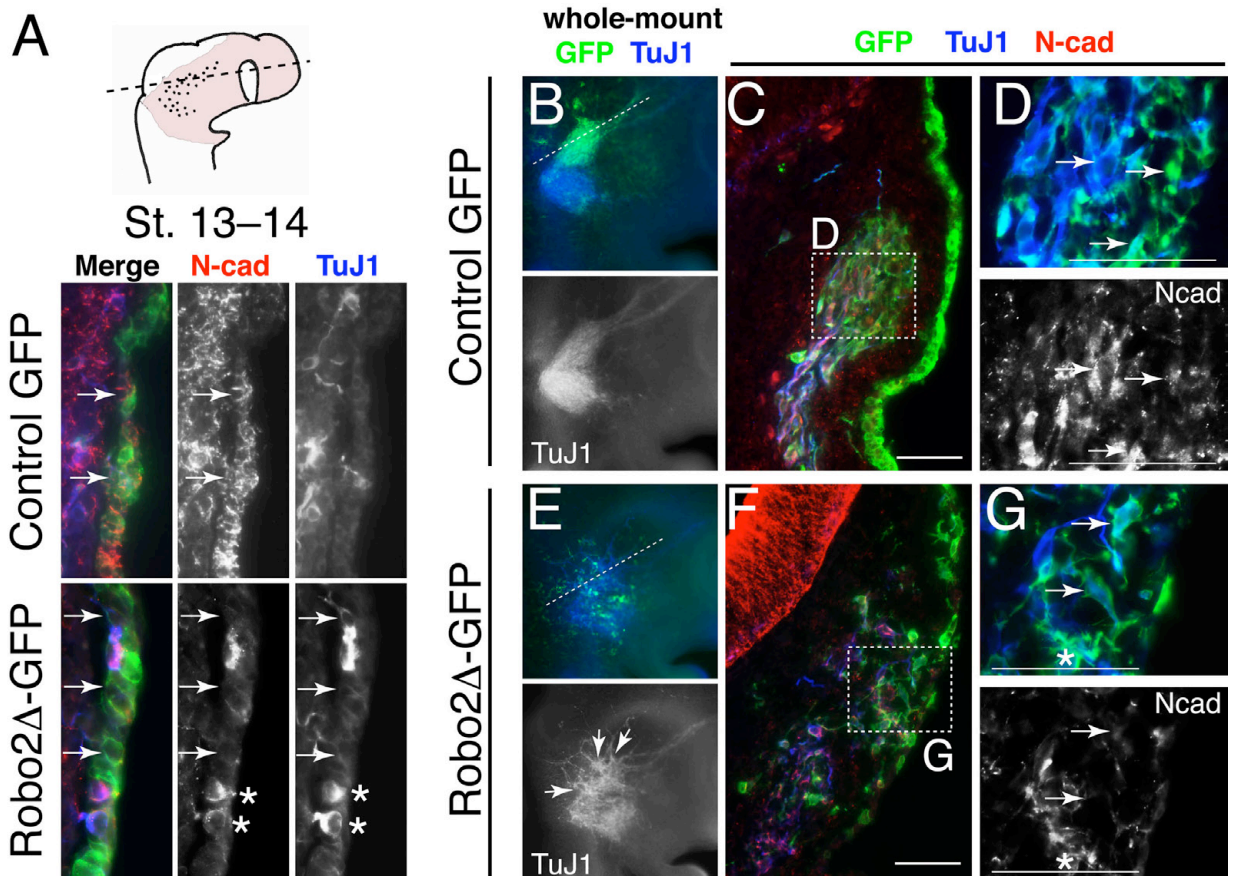
A
St. 13–14
Merge
N-cad
TuJ1
Control GFP
Robo2Δ-GFP
whole-mount
GFP TuJ1
GFP TuJ1 N-cad
B
C
D
E
F
G
TuJ1
Ncad

Figure 6. Blocking Robo2 function can downregulate N-cadherin expression in placodes. (**A**) Cross section through the OpV in stages 13–14 control GFP embryos shows N-cadherin expression in the placodal ectoderm and ingressing placodal cells labeled by TuJ1 (arrows). However, Robo2Δ-GFP placodal cells at the same stages and region have lower intensity of N-cadherin immunostaining in the placodal ectoderm (arrows), though some TuJ1 expressing placodal cells in the ectoderm still retain some levels of N-cadherin (asterisks). Later in the forming ganglion at stage 16, (**B**) control GFP placodal cells coalesce normally into ganglion. (**C**) In a section through the OpV indicated in **B**, these GFP expressing placodal neurons express N-cadherin (**D,** arrows). However, (**E**) Robo2Δ-GFP placodal neurons do not assemble properly. (**F**) In a section at the level shown in **E**, they appear abnormally disorganized with aberrant axonal projections and these individual cells that appear more dispersed have markedly reduced N-cadherin expression (**G,** arrows). Some Robo2Δ-GFP cell clusters still express N-cadherin (**G,** asterisk). Scale bars, 100 μm in C and F, and 50 μm in D and G. OpV, ophthalmic.

Figure 7.

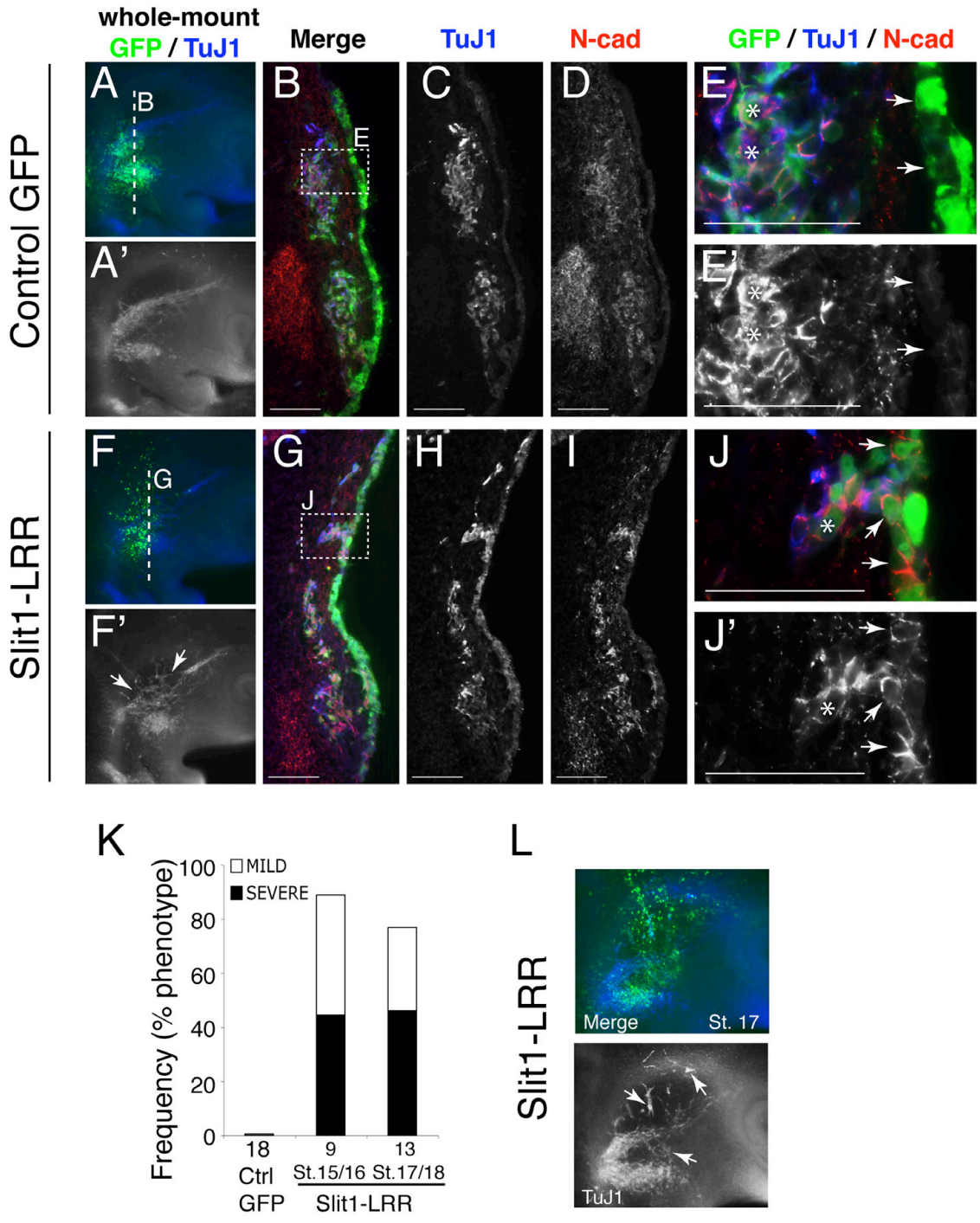
whole-mount
GFP / TuJ1
Merge
TuJ1
N-cad
GFP / TuJ1 / N-cad
Control GFP
Slit1-LRR
A
A'
B
C
D
E
E'
F
F'
G
H
I
J
J'
K
Frequency (% phenotype)
100
80
60
40
20
0
MILD
SEVERE
18
9
13
Ctrl
GFP
St.15/16 St.17/18
Slit1-LRR
L
Slit1-LRR
Merge
St. 17
TuJ1

Figure 7. Slit1 overexpression causes upregulation of N-cadherin expression in the placodal ectoderm. In stage 16 control GFP embryos shown in (**A**) color overlay of GFP (green) and TuJ1 (blue) and (**A'**) TuJ1 single channel. (**B–D**) Section at the level indicated by the dotted line in **A** shows proper coalescence of placodal cells in both OpV and MmV regions. (**E**,**E'**) High magnification of boxed region in **B** showing that N-cadherin is highly expressed by ingressed and condensing placodes (asterisks), but down-regulated in the placodal ectoderm which has no or little N-cadherin expression (arrows). By contrast, (**F**, **F'**) Slit1-LRR expressing placodal cells do not assemble properly into ganglion and appear to aberrantly aggregate at stage 16. (**G–I**) Section at the level indicated by the dotted line in **F** shows that these placodal neurons aberrantly cluster and sometimes remain in contact with the surface ectoderm. (**J**,**J'**) High magnification image of boxed region in **G** shows that in these abnormal placodal clusters, placodal cells (TuJ1+) have markedly increased N-cadherin expression in the surface ectoderm (arrows), where N-cadherin is normally down-regulated, and ingressed placodes also express N-cadherin (asterisks). (**K**) Histogram of data shows that the frequency of aberrant ganglionic aggregations is significant in Slit1-LRR embryos though the stages of gangliogenesis (stages 15–18). (**L**) At later stages 17–18, ectopic placodal neuronal clusters and abnormal placodal coalescence were found in Slit1-LRR embryos (arrows). Scale bars, 100 μm in B–D and G–I, and 50 μm in E, E', J, and J'.

Figure 8.

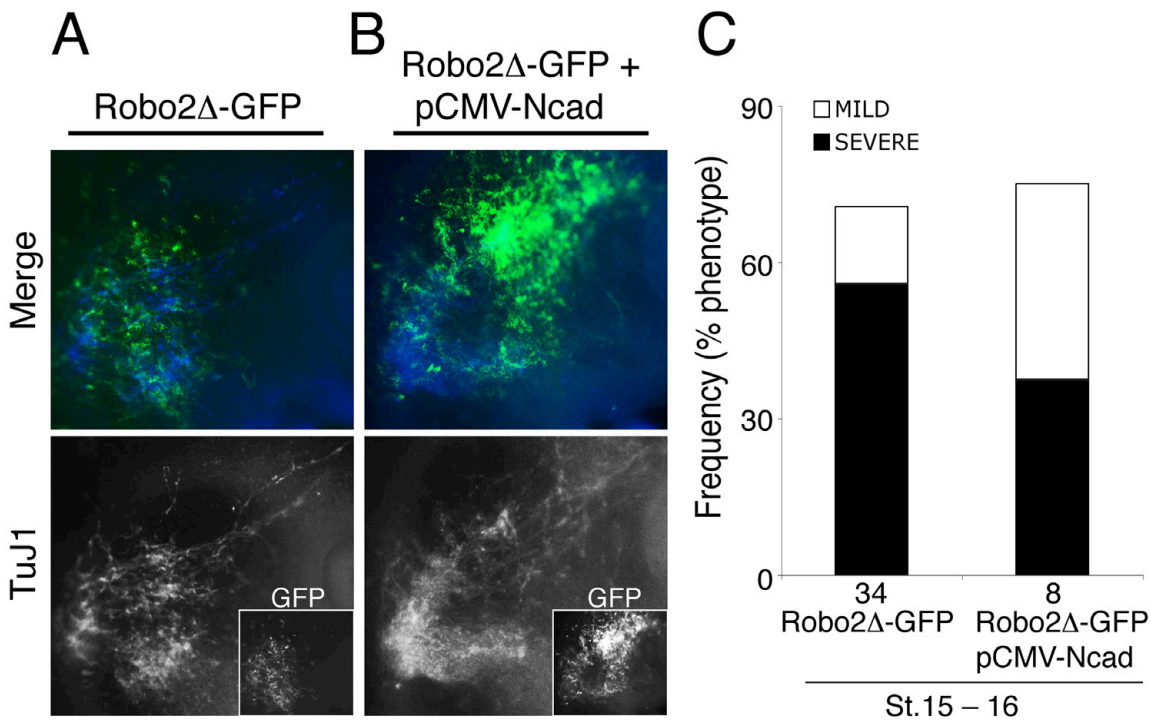

Figure 8. Full-length N-cadherin partially rescues effects of Robo2 inhibition. (**A**) The severe effects of Robo2Δ-GFP causing severely disorganized and dispersed placodal ganglia can be suppressed by (**B**) coexpression of full-length N-cadherin, which leads to more coalesced ganglia. Insets, GFP expression showing region of transfection. (**C**) Histogram of data shows that co-electroporating full-length N-cadherin and Robo2Δ-GFP markedly reduces the severe effects of Robo2Δ-GFP. Numbers below bar graphs represent the number of transfected ganglia analyzed.

Figure 9.

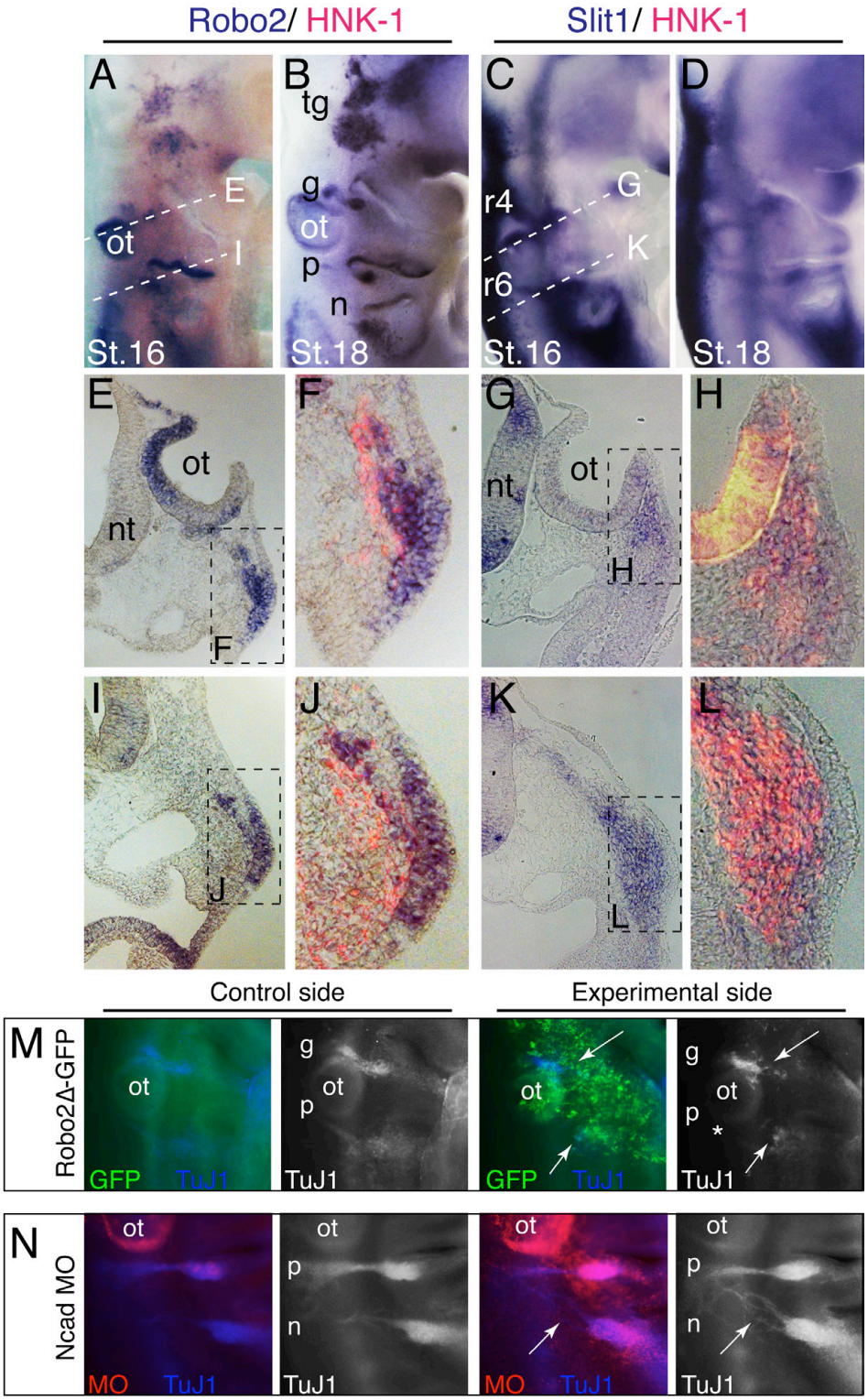
Robo2/ HNK-1
Slit1/ HNK-1
A
B
tg
g
ot
p
n
E
I
St.16
St.18
C
D
r4
G
K
r6
St.16
St.18
E
ot
nt
F
F
G
ot
nt
H
H
I
J
J
K
L
L
Control side
Experimental side
M
Robo2Δ-GFP
ot
GFP
TuJ1
g
ot
p
TuJ1
ot
GFP
TuJ1
g
ot
p
*
TuJ1
N
Ncad MO
ot
MO
TuJ1
ot
p
n
TuJ1
ot
MO
TuJ1
ot
p
n
TuJ1

Figure 9. Expression of Robo2 and Slit1, and the functions of Robo2 and N-cadherin in the forming epibranchial ganglia suggest a common mechanism underlying neural crest–placode interaction during cranial gangliogenesis. Robo2 mRNA is expressed in all the epibranchial placodes shown (**A**) at early ganglia assembly at stage 16 and (**B**) persists in the condensing ganglia at stage 18. Hindbrain neural crest streams at rhombomeres 4 and 6 that intermingle with epibranchial placodes concurrently express Slit1 mRNA (**C**) during ganglia assembly at stage 16 but (**D**) begin to downregulate Slit1 in the condensed ganglia by stage 18. (**E**) Cross section at stage16 at the level indicated in **A** shows Robo2 expression in the otic vesicle and in both ectodermal and ingressing geniculate placodes, which (**F**) is complementary to the HNK-1 expression by neural crest cells that (**G**,**H**) are expressing Slit1. Similarly, (**I**) petrosal placodes express Robo2 in the surface ectoderm and during ingression at stage 16 as shown in a cross section at the level indicated in **A** and (**J**) associate with HNK-1+ neural crest cells (**K**,**L**) that express Slit1. (**M**) Compared to the control side with no DNA transfection, the Robo2Δ-GFP electroporated epibranchial ectoderm of the same stage 15 embryo showed severely disorganized geniculate and petrosal placodal ganglia (arrows), and reduction or loss of axonal projections to the hindbrain by the forming petrosal ganglion (asterisk). (**N**) In contrast to the control side with no transfection in the nodose ganglion, knockdown of N-cadherin by Ncad MO caused disorganization of the nodose placodal neurons, namely their central axonal projections at stage 17 (arrow). ot, otic vesicle; tg, trigeminal; g, geniculate; p, petrosal; n, nodose; r4, rhombomere 4; r6, rhombomere 6; nt, neural tube.